Journal of Management Practices, Humanities and Social Sciences
ISSN: 2604-6423, Volume 12, Issue 3, 121-132

AI-BASED OPTIMIZATION OF SOLAR-ASSISTED GREEN HYDROGEN PRODUCTION AND STORAGE USING CASSAVA PEEL-DERIVED ACTIVATED BIOCHAR IN IBADAN, NIGERIA

Idowu Olugbenga Adewumi[1], Wumi Ajayi[2], Akintayo Ayoade[3], Tolulope Olufemi[4], Oluwafisayo Babatope Ayoade[5], Kikelomo Ibiwumi Okesola[6] Azeez Ajani Waheed[7]

[1]*Software Engineering Program, Department of Computer and Information Engineering, Faculty of Natural and Applied Science, Lead City University, Ibadan, Oyo State, Nigeria.*

[2]*Software Engineering Department, School of Computing, Babcock University, Nigeria.*

[3]*Department of Computer and Information Engineering, Faculty of Natural and Applied Science, Lead City University, Ibadan, Oyo State, Nigeria*

[4]*Department of Computer and Information Engineering, Faculty of Natural and Applied Science, Lead City University, Ibadan, Oyo State, Nigeria.*

[5]*School of Computer, Data and Mathematical Sciences, Computing and Engineering, Western Sydney University, Australia.*

[6]*Software Engineering Department, School of Computing, Babcock University, Ogun State, Nigeria*

7*Department of Computer Science, Faculty of Natural and Applied Science, Lead City University, Ibadan Nigeria*

Abstract

This study designed a framework to optimize the production and potential storage of green hydrogen using activated biochar from cassava peel. Cassava peel biochar was produced via pyrolysis and activation and evaluated for a function material for alkaline water electrolysis and hydrogen storage. The biochar yield of the activated biochar is 39.28 ± 4.32%; fixed carbon content is 71.59 ± 4.50%. BET surface area is 860.00 ± 290.00 m^2/g; pore volume is 0.45 ± 0.15 cm^3/g; electrical conductivity is 1.47 ± 0.75 mS/cm. The use of KOH as the activation agent yielded the highest BET surface area (976.00 m^2/g) and pore volume (0.51 cm^3/g). The maximum hydrogen production of 2380.00 mL at a production rate of 25.10 mL/min at 0.91-1.55 M KOH was achieved with Faradaic efficiency of 86.20% and energy efficiency of 64.10%. As the pressure increased from 1 bar to 30 bar, the quantity of hydrogen absorbed increased from 0.65 wt.% to 1.23 wt.%. The desorption efficiency dropped from 81.30% to 74.10%. XGBoost was the model which predicted the best, with an R^2 of 0.96, RMSE of 1.78, MAE of 1.21, MAPE of 6.40% and a classification accuracy of 0.94. The predicted hydrogen production from the optimized conditions was 48.60 mL/min which gives 78.40% energy efficiency which gave hydrogen uptake of 1.52 wt.%. The innovative research illustrates a relevant local pathway to biomass-based green hydrogen systems.

Keyword: Green hydrogen; Cassava peel biochar; Solar-assisted electrolysis; Hydrogen storage; Artificial intelligence optimization

---

Date of acceptance: 02-04-2026 Date of Publication: 27-05-2026

Graphical Abstract

Journal of Management Practices, Humanities and Social Sciences
ISSN: 2604-6423, Volume 12, Issue 3, 121-132

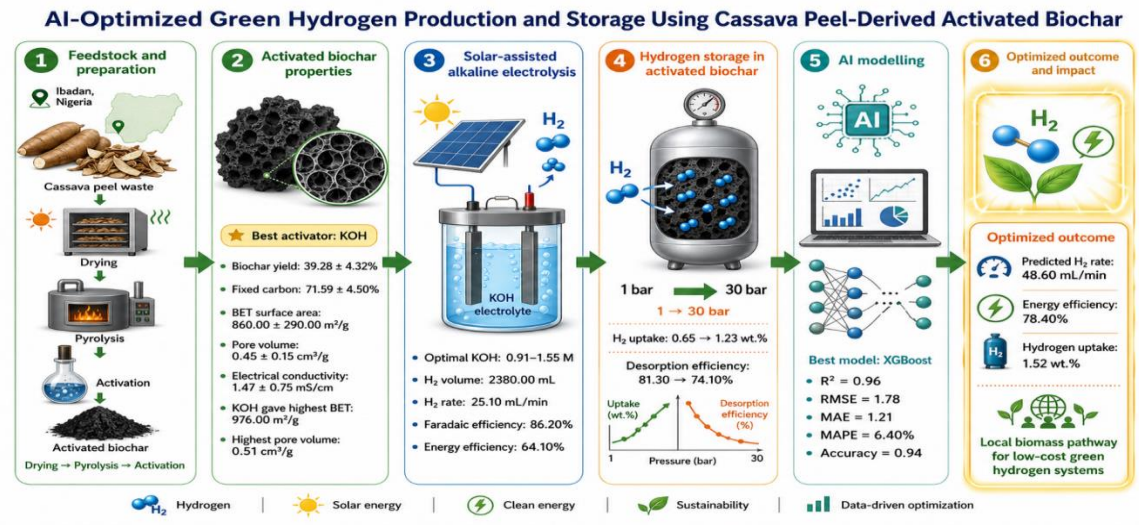

I. INTRODUCTION

Green hydrogen is increasingly being seen as a key energy carrier for the decarbonisation of power, transport, industrial heat, fertiliser production, and long-duration renewable energy storage. Nevertheless, the world hydrogen production remains largely fossil fuel-based. According to the International Energy Agency (IEA) (2024), global hydrogen production reached around 97 Mt in 2023, but low-emission hydrogen accounted for less than 1% of that amount. This article shows that the transition from conventional hydrogen to renewable hydrogen is still at an early phase. Moreover, the production of renewable hydrogen is more expensive compared to fossil-based hydrogen due to high electricity requirements, electrolyser costs, material limitations and safe and efficient storage (IEA, 2024). These constraints receive particular importance in developing economies where imported materials, unstable grid electricity (and the complexities stemming from it), and limited research infrastructure increase costs.

There is a need for locally adaptable green hydrogen research in Nigeria due to energy transition. The new Nigeria Energy Transition and Investment plan flags large-scale renewable power expansion, energy storage and new energy technologies, including hydrogen infrastructure, to power the country's net-zero pathway by 2060 (Sustainable Energy for All, 2024). Nonetheless a big problem is that most hydrogen production technologies are designed around expensive imported catalysts, membranes, storage materials, and high-end lab materials. This restricts their practical use in local settings in Nigeria, especially where low-cost, decentralised and renewable energy systems are needed.

The method of alkaline water electrolysis which is assisted by solar is considered as a promising option as it takes up photovoltaic electricity in order to split water into hydrogen and oxygen. Recent research indicates that the use of photovoltaic energy in alkaline water electrolysis can enhance the sustainable hydrogen production, however, a wide array of parameters such as solar irradiance, electrolyser design, catalyst behaviour, electrolyte concentration, current density, temperature, and operational fluctuations affect the system performance (Tello Zamorano et al. 2025). As a result, utilizing inexpensive materials and smart optimization of operating conditions can improve the efficiency of the process.

The effective use of hydrogen for green energy is stalled largely by its storage problem. Storage systems need to be efficient, safe, cheap and stable. Recent reviews identified carbonaceous materials derived from biomass as a promising alternative for hydrogen storage owing to their renewable waste resource and high surface area, tunable porosity and adjustable surface functional groups (Khan et al., 2025). Nevertheless, the performance of these materials is strongly dependent on biomass type, pyrolysis temperature, method of activation, pore structure, surface chemistry, and post-treatment conditions.

Relevant to Ibadan and Oyo State, cassava processing generates substantial peel residues that are often wasted. Nigeria leads the world in cassava production, with an output of about 63 million tonnes, representing about 31% of production in Africa and 20% globally (Otekunrin et al., 2024). Recent investigations on the cassava-processing centres in Oyo State have further shown the environmental relevance of the peels and effluents from local processing activities (Olaniyan et al., 2025). As such, cassava peel waste is a locally accessible carbon-rich biomass that is suitable for producing activated biochar for energy applications.

There are still three prominent gaps in the growing literature on green hydrogen. Most hydrogen production studies focus on either advanced electrolyser materials, commercial catalysts or costly imported components.

However, not much work has been done on the utilization of locally available agricultural residues as functional materials for low-cost hydrogen system in Nigeria. The implication of this is a local applicability gap where technologies that work efficiently in advanced laboratories are not necessarily economically or technically viable for Ibadan, and similar contexts.

Also, while the use of carbon materials derived from biomass has received increased attention as candidates for hydrogen storage, the specific use of cassava peel-derived activated biochar as a dual-purpose support for green hydrogen production and storage assessment is less studied. According to recently published articles, carbon materials which are derived from biomass can be used for hydrogen storage (Khan et al., 2025). Although the potential is there, the challenges relating to issues of scalability, structural stability, cost effectiveness and the linking of synthesis parameters to storage performance need to be addressed. This indicates the need for site-specific studies that relate the biomass conversion to materials characterization, hydrogen yield and storage capacity and process optimization.

Many experimental studies on hydrogen still rely on trial and error for optimization. Nonetheless, there are numerous variational parameters coinciding with hydrogen production and storage which include pyrolysis temperature, activation time, electrolyte concentration, voltage, current density, electrolysis duration, temperature, biochar dosage, surface area and pore volume. Traditional experimentation while fixing other variables lacks depth of interaction. Recent studies reveal that machine learning can assist with high-dimensional optimization for hydrogen systems. Zhao et al. (2025) have shown that machine learning can predict and optimize the performance of alkaline water electrolysis membranes, while Hassan and Kazemi (2025) indicated that multi-variable data-driven soft computing models can characterize the complex input–output relationship. 39 words 802 chars These investigations validate that artificial intelligence can help advance our hydrogen research, but it has hardly been applied on cassava peel biochar and solar-assisted alkaline electrolysis in Nigeria.

To mitigate the aforementioned gaps, the current study proposes an Artificial Intelligence-based optimization framework for solar-assisted green hydrogen production and storage based on cassava peel-derived activated biochar in Ibadan, Nigeria. The application of the proposed approach will convert locally available cassava peel waste into activated biochar through pyrolysis under restricted air supply and activation. The material produced will be characterized for surface morphology, functional groups, crystallinity, surface area, and porosity, pH, electrical conductivity, and carbon. It will then be examined for its economic feasibility as a substrate for evaluating solar-assisted alkaline water electrolysis and hydrogen storage.

The research will merge experimental hydrogen generation with AI modeling. Operating variables such as voltage, current density, electrolyte concentration, electrolysis time, temperature, biochar loading, activation condition, and surface properties of the material will be model inputs. The output variables will include hydrogen yield, hydrogen production rate, energy efficiency, Faradaic efficiency, hydrogen uptake, and storage performance. In order to forecast system performance, machine learning models such as artificial neural networks, random forest, XGBoost, support vector regression and gradient boosting will be developed. The optimally performing model will be integrated with an optimization algorithm to find the best operating conditions for a maximum hydrogen yield at higher energy efficiency with better storage capacity.

This study is novel as it incorporates four components as local cassava peel valorisation with solar-assisted alkaline electrolysis, activated biochar-based hydrogen storage assessment and process optimisation with AI. It is projected that this combination will provide a low-cost and locally adaptable pathway for green hydrogen development in Ibadan, Nigeria. The study also contributes to circular bioeconomy thinking through converting an available agricultural residue into a useful energy material. Essentially, the work will back decentralised hydrogen production – renewable energy storage, waste-to-energy innovation and sustainable energy technology development in Nigeria.

II. MATERIALS AND METHODS

2.1 Study Design

This study adopted an experimental and computational design to optimize solar-assisted green hydrogen production and hydrogen storage using cassava peel-derived activated biochar. The work combined biomass conversion, biochar activation, alkaline water electrolysis, hydrogen storage assessment, and artificial intelligence-based optimization. The experimental component focused on the preparation and characterization of cassava peel-derived activated biochar, while the computational component used machine learning models to predict hydrogen production rate, energy efficiency, hydrogen uptake, and overall system performance.

The study was structured around three main phases. First, cassava peel residues were processed into activated biochar through drying, pyrolysis, and activation. Second, the activated biochar was evaluated within a solar-assisted alkaline electrolysis system for green hydrogen production and storage assessment. Third, the resulting

multivariable dataset was used to train and evaluate machine learning models for process prediction and optimization.

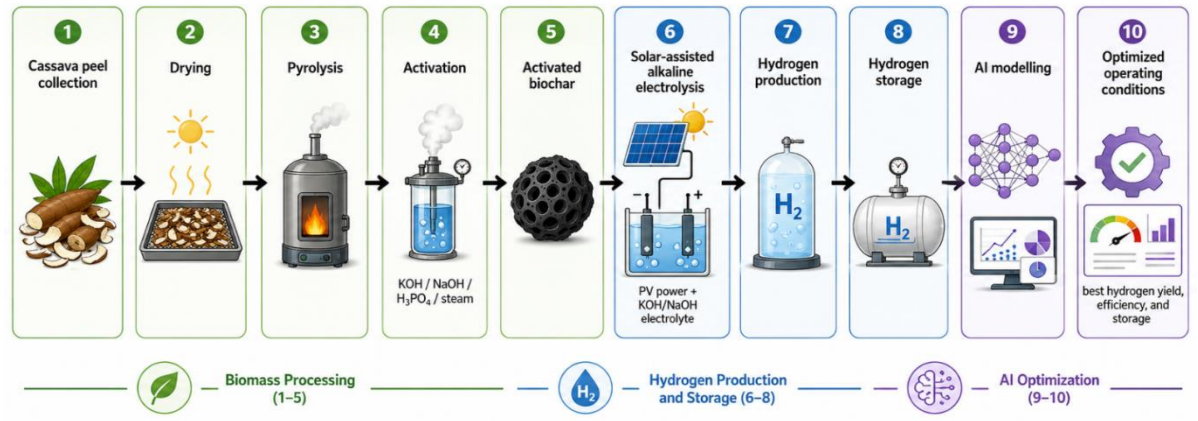

Figure 2.1: Integrated Workflow of Cassava Peel Conversion, Hydrogen Production, Storage, and AI Optimization

2.2 Study Location

The experimental work was conducted at **AAT Workshop and Laboratory, Odo-Ona Elewe Area, Ibadan, Oyo State, Nigeria**. Ibadan was selected because of its high availability of cassava processing residues, favourable solar radiation conditions, and growing relevance for decentralized renewable energy research. Cassava peel was selected as the biomass feedstock because it is locally available, low-cost, and commonly generated as an agricultural and food-processing residue in the study area.

2.3 Biomass Collection and Preparation

Cassava peel residues were obtained from cassava processing points within Ibadan, Oyo State. The collected biomass was manually sorted to remove stones, soil particles, plastics, and other unwanted materials. The peels were washed with clean water to remove surface impurities and then dried using sun-drying, oven-drying at 60°C, or hybrid solar drying, depending on the experimental condition.

After drying, the cassava peels were ground and sieved into different particle-size fractions. The particle sizes considered in the experimental design included **150, 250, 355, 500, 710, and 1000 µm**. The prepared biomass was stored in airtight containers before pyrolysis to prevent moisture reabsorption.

2.4 Production of Cassava Peel-Derived Biochar

Cassava peel-derived biochar was produced through controlled pyrolysis under limited oxygen conditions. The pyrolysis temperature ranged from **400°C to 750°C**, while the residence time ranged from **45 to 180 minutes**. These operating ranges were selected to evaluate the influence of carbonization severity on biochar yield, fixed carbon content, pore development, and subsequent hydrogen production performance.

After pyrolysis, the biochar was allowed to cool to room temperature under oxygen-limited conditions. Biochar yield was calculated as:

$$\text{Biochar yield}(\%) = \frac{\text{Mass of biochar after pyrolysis}}{\text{Initial dry mass of cassava peel}} \times 100$$

The produced biochar was stored in labelled airtight containers prior to activation and characterization.

2.5 Biochar Activation

The cassava peel-derived biochar was activated to improve its surface area, pore volume, conductivity, and potential performance as an electrode-support and hydrogen storage material. The activation agents considered were **KOH, NaOH, H_3PO_4, steam, and non-activated control treatment**.

For chemical activation, biochar was mixed with the selected activating agent at different impregnation ratios. The activation ratio ranged from **0.5:1 to 3:1 w/w**, while activation temperature ranged from **500°C to 850°C**. Activation time ranged from **30 to 150 minutes**. After activation, chemically treated biochar samples were washed repeatedly with distilled water until near-neutral pH was achieved. The samples were then dried and stored for further use.

2.6 Characterization of Activated Biochar

The activated biochar samples were characterized to determine their physicochemical and structural properties and to assess their suitability for green hydrogen production and storage applications. The characterization focused on parameters that influence electrochemical activity, surface interaction, adsorption capacity, and overall material performance. These included biochar yield, ash content, volatile matter, fixed carbon, pH, electrical conductivity, elemental composition, surface area, pore volume, and average pore diameter.

Proximate analysis was carried out to determine the moisture content, ash content, volatile matter, and fixed carbon content of the cassava peel-derived activated biochar. These parameters were important because they provided information on the stability, carbon richness, and combustion-related properties of the prepared material. A higher fixed carbon content was considered desirable because it indicates improved carbonization and better potential for conductivity and adsorption-related applications.

The pH and electrical conductivity of the activated biochar were measured using standard aqueous suspension methods. The pH value was used to assess the acidic or alkaline nature of the biochar surface, while electrical conductivity was used to evaluate its potential contribution to electron transfer during electrolysis. These properties are important because surface chemistry and conductivity can influence the performance of biochar when used as an electrode-support or functional material in hydrogen production systems.

The surface area and pore structure of the activated biochar were evaluated using Brunauer–Emmett–Teller analysis. This analysis provided information on the BET surface area, pore volume, and average pore diameter of the material. These properties were essential for assessing the hydrogen storage potential of the activated biochar, since materials with suitable porosity and larger accessible surface area are generally more favourable for gas adsorption and storage.

Elemental composition was also determined to quantify the relative proportions of carbon, oxygen, hydrogen, and nitrogen in the activated biochar. The carbon content was particularly important because it reflected the quality of carbonization and the suitability of the material for energy-related applications. Oxygen-, hydrogen-, and nitrogen-containing functional groups were also considered relevant because they may influence surface reactivity, adsorption behaviour, and interaction with electrolyte species during electrolysis.

The characterization results were later used as input variables for model development. Specifically, biochar yield, ash content, volatile matter, fixed carbon, BET surface area, pore volume, average pore diameter, biochar pH, electrical conductivity, and elemental composition were incorporated into the artificial intelligence-based optimization framework to predict hydrogen yield, energy efficiency, hydrogen uptake, and overall system performance.

2.7 Solar-Assisted Alkaline Water Electrolysis Setup

Green hydrogen production was conducted using a solar-assisted alkaline water electrolysis system designed to evaluate the effect of renewable electricity and cassava peel-derived activated biochar on hydrogen generation. The setup consisted of a photovoltaic panel, charge controller, direct current power regulation unit, alkaline electrolysis cell, electrode assembly, electrolyte chamber, gas collection unit, and hydrogen measurement system. The system was arranged to allow solar energy to provide the electrical input required for water splitting under alkaline conditions.

The photovoltaic panel served as the main power source for the electrolysis process. Electricity generated from the panel was regulated through the charge controller and direct current regulation unit before being supplied to the electrolysis cell. This was necessary to ensure stable voltage and current delivery during the experimental runs. The solar-assisted design was adopted to reduce dependence on grid electricity and to support the production of hydrogen using a renewable energy source.

The alkaline electrolysis cell contained the electrolyte solution, electrode assembly, and biochar-assisted component. Potassium hydroxide or sodium hydroxide was used as the alkaline electrolyte because both electrolytes improve ionic conductivity and facilitate hydrogen and oxygen evolution reactions. The electrolyte concentration varied from **0.25 M to 2.20 M** in order to determine the effect of electrolyte strength on hydrogen production performance. The activated biochar produced from cassava peel was incorporated as a functional material to assess its contribution to electrochemical performance and hydrogen generation efficiency.

During each experimental run, key environmental and electrical parameters were monitored. Solar irradiance, ambient temperature, relative humidity, panel temperature, panel voltage, panel current, and solar power output were recorded to evaluate the influence of solar conditions on electrolysis performance. These parameters were important because variations in solar intensity and panel temperature can affect power output, cell voltage, current density, and overall hydrogen yield.

The electrolysis operating conditions were also measured and recorded throughout the experiment. These included electrolyte type, electrolyte concentration, electrolysis voltage, current density, electrolysis temperature, electrolysis time, electrode area, and biochar loading. These variables were selected because they

directly influence hydrogen production rate, energy consumption, Faradaic efficiency, and overall system efficiency.

All recorded solar, electrochemical, and material-related variables were later used for artificial intelligence-based modelling and optimization. The integration of solar input data, electrolyte conditions, electrode parameters, and biochar loading made it possible to evaluate the combined effect of renewable power supply and activated biochar on green hydrogen production. This setup therefore provided a practical basis for optimizing low-cost solar-assisted alkaline electrolysis using locally derived cassava peel biochar in Ibadan, Nigeria.

2.8 Hydrogen Production Measurement

Hydrogen production was evaluated by measuring the volume of gas generated during electrolysis. The hydrogen volume was recorded in millilitres, while hydrogen production rate was calculated as the volume of hydrogen produced per unit time.

$$\text{Hydrogen production rate} = \frac{\text{Hydrogen volume produced}}{\text{Electrolysis time}}$$

Energy consumption was estimated based on the applied voltage, current density, electrode area, and electrolysis duration. Energy efficiency and Faradaic efficiency were calculated to assess the conversion performance of the electrolysis system.

The main hydrogen production outputs were:

i. Hydrogen volume
ii. Hydrogen production rate
iii. Energy consumption
iv. Faradaic efficiency
v. Energy efficiency

2.9 Hydrogen Storage Assessment

The hydrogen storage potential of cassava peel-derived activated biochar was assessed by evaluating hydrogen uptake, desorption efficiency, and capacity retention under different storage conditions. The storage pressure levels considered were **1, 5, 10, 20, and 30 bar**, while storage temperature was recorded for each experimental condition.

Repeated adsorption–desorption cycles were used to assess material reusability. The storage cycle number ranged from **1 to 30 cycles**. Hydrogen uptake was expressed as weight percentage, while desorption efficiency and capacity retention were expressed as percentages.

The hydrogen storage outputs included:

i. Hydrogen uptake
ii. Desorption efficiency
iii. Storage cycle number
iv. Capacity retention
v. Storage pressure
vi. Storage temperature

2.10 Dataset Description

The final dataset contained **50,000 experimental records** and **57 variables** covering biomass preparation, biochar production, activation conditions, material characterization, solar-assisted electrolysis, hydrogen production, hydrogen storage, and machine learning target variables.

The dataset included the following categories of variables:

Table 2.1: Dataset Description

Category	Examples of variables
Biomass source and preparation	Biomass source, drying method, particle size
Pyrolysis and activation	Pyrolysis temperature, pyrolysis time, activation agent, activation ratio
Biochar properties	BET surface area, pore volume, fixed carbon, pH, conductivity
Solar conditions	Irradiance, ambient temperature, humidity, panel voltage, panel current

Electrolysis conditions	Electrolyte type, concentration, voltage, current density, time
Hydrogen production outputs	Hydrogen volume, production rate, energy efficiency, Faradaic efficiency
Storage outputs	Hydrogen uptake, desorption efficiency, capacity retention
AI targets	Performance score, performance class, optimum candidate flag

For Scopus submission, the origin of the dataset must be clearly stated. If the dataset was generated computationally, it should be described as a **synthetic experimental dataset**. If the values were measured at AAT Workshop and Laboratory, then laboratory records, instrument logs, calibration records, and raw measurement sheets should be retained for verification.

2.11 Machine Learning Model Development

Machine learning models were developed to predict hydrogen production and storage performance from the experimental variables. The input variables included pyrolysis temperature, activation temperature, activation time, activation ratio, BET surface area, pore volume, electrolyte concentration, electrolysis voltage, current density, electrolysis temperature, electrolysis time, solar irradiance, panel voltage, panel current, and biochar loading.

The target variables were:

i. Hydrogen volume
ii. Hydrogen production rate
iii. Energy efficiency
iv. Hydrogen uptake
v. Performance score
vi. Performance class
vii. Optimum candidate flag

Both regression and classification models were developed. Regression models were used to predict continuous outputs, while classification models were used to classify system performance as low, moderate, or high. The candidate models included Random Forest, XGBoost, Gradient Boosting, Support Vector Regression, and Artificial Neural Network models.

2.12 Data Preprocessing

Before model training, the dataset was cleaned and preprocessed. Missing values were examined and treated using appropriate imputation methods. Continuous variables were standardized or normalized where required. Categorical variables, including activation agent, electrolyte type, drying method, water source, biomass source, and electrolysis cell type, were encoded using suitable categorical encoding methods.

Outliers were screened using descriptive statistics and distributional checks. The dataset was then divided into training, validation, and testing subsets. A typical split of **70% training, 15% validation, and 15% testing** was used to evaluate model generalizability.

2.13 Model Evaluation

The performance of the regression models was evaluated using standard statistical error and goodness-of-fit metrics. The coefficient of determination was used to determine how well each model explained the variation in the target outputs, including hydrogen production rate, energy efficiency, hydrogen uptake, and capacity retention. Root mean square error and mean absolute error were used to quantify the magnitude of prediction errors, while mean absolute percentage error was used to express prediction error in percentage terms. These metrics provided a balanced assessment of model accuracy, error size, and predictive reliability.

For the classification tasks, model performance was evaluated using accuracy, precision, recall, F1-score, confusion matrix, and receiver operating characteristic–area under the curve where applicable. Accuracy was used to measure the overall proportion of correct classifications, while precision and recall were used to assess the model's ability to correctly identify high-performing and low-performing system conditions. The F1-score provided a balanced measure of precision and recall, especially where class distribution differed across performance categories. The confusion matrix was used to examine correct and incorrect classifications across low, moderate, and high performance groups.

The best-performing model was selected based on a combination of predictive accuracy, low error values, interpretability, and stability across validation runs. For regression outputs, preference was given to models with

higher coefficient of determination and lower root mean square error, mean absolute error, and mean absolute percentage error. For classification outputs, preference was given to models with higher accuracy, precision, recall, F1-score, and ROC-AUC values. Model interpretability was also considered important because the study aimed not only to predict hydrogen production and storage performance, but also to identify the key variables influencing system optimization.

2.14 Optimization Procedure

The best-performing machine learning model was used for process optimization after model training and evaluation. The main objective of the optimization procedure was to identify the most suitable operating conditions for maximizing hydrogen production rate, energy efficiency, hydrogen uptake, and capacity retention, while minimizing energy consumption. This approach was adopted to ensure that the selected conditions were not only technically efficient but also practical for low-cost green hydrogen production and storage using cassava peel-derived activated biochar.

The optimization process considered both material preparation and electrolysis operating variables. The material-related variables included pyrolysis temperature, activation temperature, and activation ratio, because these factors influence the surface area, pore structure, conductivity, and adsorption capacity of the activated biochar. The electrolysis-related variables included electrolyte concentration, electrolysis voltage, current density, electrolysis time, and biochar loading, as these directly affect hydrogen generation, Faradaic efficiency, and energy consumption. Storage-related variables included storage pressure and storage temperature, which were included because they influence hydrogen uptake, desorption behaviour, and capacity retention.

The optimized results were used to identify candidate operating conditions that produced the best balance between hydrogen yield, energy efficiency, and storage performance. The final optimum conditions were selected by considering the combined performance of hydrogen production and storage indicators rather than relying on a single output variable. This multi-output approach ensured that the recommended conditions were suitable for practical application and could support the development of an efficient solar-assisted green hydrogen system using locally available cassava peel biomass in Ibadan, Nigeria.

2.15 Data Integrity and Reproducibility

All experimental runs were assigned unique identification codes. Data were organized in comma-separated values format and checked for consistency before analysis. The dataset contained labelled variables, unit descriptions, input parameters, output indicators, and machine learning targets to ensure reproducibility.

For publication purposes, the dataset should be accompanied by a data dictionary, preprocessing script, and model-development code. Where synthetic or simulated values are used, this must be explicitly disclosed in the manuscript to maintain research transparency and publication integrity.

2.16 Ethical and Safety Considerations

The study did not involve human or animal subjects. However, laboratory safety precautions were followed during pyrolysis, chemical activation, alkaline electrolysis, and hydrogen handling. Chemical activation agents such as KOH, NaOH, and H_3PO_4 were handled using gloves, laboratory coats, eye protection, and proper ventilation. Hydrogen was collected and handled away from ignition sources due to its flammability. Waste chemicals were neutralized and disposed of according to standard laboratory safety procedures.

III. DEVELOPED MATHEMATICAL MODEL FRAMEWORK FOR THE STUDY

3.1.1Overview of the Model

To describe the interrelationship among cassava peel-derived activated biochar preparation, solar-assisted alkaline water electrolysis, hydrogen production, hydrogen storage and artificial intelligence-based optimization a mathematical model was developed. Five components were modelled which presented an interconnected modelling framework that determines biomass to biochar, solar power input estimation, hydrogen production through alkaline electrolysis, hydrogen storage performance, and prediction and optimisation using machine learning.

The general relationship between the input variables and the target outputs was expressed as:

$$Y = f(X) + \varepsilon \qquad (3.1)$$

where Yrepresents the target response variables, Xrepresents the vector of experimental and process input variables, $f(X)$is the unknown nonlinear function learned by the artificial intelligence models, and εrepresents the random error term associated with measurement variation and process uncertainty.

The input vector for each experimental run was defined as:

$$X_i = [T_p, t_p, A_r, T_a, t_a, C_e, V_e, J, T_e, t_e, B_L, G, P_s, P_{st}, T_{st}] \qquad (3.2)$$

where $T_p$is pyrolysis temperature, $t_p$is pyrolysis time, $A_r$is activation ratio, $T_a$is activation temperature, $t_a$is activation time, $C_e$is electrolyte concentration, $V_e$is electrolysis voltage, $J$is current density, $T_e$is electrolysis temperature, $t_e$is electrolysis time, $B_L$is biochar loading, $G$is solar irradiance, $P_s$is solar power output, $P_{st}$is storage pressure, and $T_{st}$is storage temperature.
The output vector was expressed as:
$Y_i = [V_{H_2}, R_{H_2}, \eta_F, \eta_E, U_{H_2}, D_e, C_r]$ (3.3)
where $V_{H_2}$is hydrogen volume, $R_{H_2}$is hydrogen production rate, $\eta_F$is Faradaic efficiency, $\eta_E$is energy efficiency, $U_{H_2}$is hydrogen uptake, $D_e$is desorption efficiency, and $C_r$is capacity retention.

3.1.2 Biochar Yield Model
The yield of cassava peel-derived biochar was calculated from the ratio of the final mass of biochar to the initial dry mass of cassava peel biomass:
$Y_b = \frac{M_b}{M_{cp}} \times 100$ (3.4)
where $Y_b$is the biochar yield in percentage, $M_b$is the mass of biochar obtained after pyrolysis, and $M_{cp}$is the initial dry mass of cassava peel.
The activated biochar properties were treated as functions of pyrolysis and activation conditions:
$B_p = f(T_p, t_p, A_g, A_r, T_a, t_a)$ (3.5)
where $B_p$represents biochar properties such as fixed carbon, ash content, volatile matter, BET surface area, pore volume, average pore diameter, pH, and electrical conductivity. $A_g$represents the activation agent, while $A_r$represents the activation ratio.
For modelling purposes, the biochar characterization vector was expressed as:
$B_p = [C_f, A_s, V_m, S_{BET}, V_p, D_p, pH_b, EC_b]$ (3.6)
where $C_f$is fixed carbon, $A_s$is ash content, $V_m$is volatile matter, $S_{BET}$is BET surface area, $V_p$is pore volume, $D_p$is average pore diameter, $pH_b$is biochar pH, and $EC_b$is electrical conductivity.

3.1.3 Solar Power Input Model
The solar-assisted electrolysis system used photovoltaic power as the main energy source. The instantaneous solar power output was calculated as:
$P_s = V_{pv} \times I_{pv}$ (3.7)

where $P_s$is the solar power output in watts, $V_{pv}$is the photovoltaic panel voltage, and $I_{pv}$is the photovoltaic panel current.
The theoretical photovoltaic output can also be expressed as:
$P_s = \eta_{pv} A_{pv} G[1 - \beta(T_{pv} - T_{ref})]$ (3.7)
where $\eta_{pv}$is the photovoltaic panel efficiency, $A_{pv}$is the panel area, $G$is solar irradiance, $\beta$is the temperature coefficient of the panel, $T_{pv}$is the panel temperature, and $T_{ref}$is the reference temperature.
The electrical energy supplied to the electrolysis cell was estimated as:
$E_{in} = \frac{V_e I_e t_e}{1000}$ (3.8)
where $E_{in}$is the electrical energy input in kilowatt-hours, $V_e$is the electrolysis voltage, $I_e$is the electrolysis current, and $t_e$is the electrolysis duration in hours.
If current density was used instead of direct current, the current was calculated as:
$I_e = \frac{J \times A_e}{1000}$ (3.9)
where $I_e$is the electrolysis current in amperes, $J$is the current density in mA/cm², and $A_e$is the electrode area in cm².

3.2 Hydrogen Production Model
Hydrogen production during alkaline water electrolysis was modelled using Faraday's law. The theoretical number of moles of hydrogen produced was calculated as:
$n_{H_2,theo} = \frac{I_e t_e}{2F}$ (3.10)
where $n_{H_2,theo}$is the theoretical number of moles of hydrogen, $I_e$is the electrolysis current, $t_e$is the electrolysis time in seconds, and $F$is Faraday's constant ($96485\ C/mol$). The denominator 2 represents the two electrons required to produce one mole of hydrogen gas.
The theoretical hydrogen volume was calculated using the ideal gas relationship:

$V_{H_2,theo} = \frac{n_{H_2,theo}RT}{P}$ (3.11)

where $V_{H_2,theo}$ is the theoretical hydrogen volume, R is the universal gas constant, T is absolute temperature, and P is pressure.

The experimental hydrogen production rate was calculated as:

$R_{H_2} = \frac{V_{H_2,exp}}{t_e}$ (3.12)

where R_{H_2} is the hydrogen production rate, $V_{H_2,exp}$ is the experimentally measured hydrogen volume, and t_e is the electrolysis time.

The Faradaic efficiency was calculated as:

$\eta_F = \frac{n_{H_2,exp}}{n_{H_2,theo}} \times 100$ (3.13)

or equivalently:

$\eta_F = \frac{2Fn_{H_2,exp}}{I_e t_e} \times 100$ (3.14)

where η_F is the Faradaic efficiency, $n_{H_2,exp}$ is the experimentally measured number of moles of hydrogen, and $n_{H_2,theo}$ is the theoretical number of moles of hydrogen.

The specific energy consumption was expressed as:

$SEC = \frac{E_{in}}{V_{H_2}}$ (3.15)

where SEC is the specific energy consumption in kWh/m³ H_2, E_{in} is the energy input, and V_{H_2} is the hydrogen volume produced.

The energy efficiency of the electrolysis system was estimated as:

$\eta_E = \frac{HHV_{H_2} \times n_{H_2,exp}}{E_{in}} \times 100$ (3.16)

where η_E is the energy efficiency, HHV_{H_2} is the higher heating value of hydrogen, $n_{H_2,exp}$ is the experimentally measured hydrogen produced, and E_{in} is the electrical energy input.

3.3 Biochar Assisted Electrolysis Response Model

The effect of cassava peel-derived activated biochar on hydrogen production was modelled as a function of biochar structural and electrochemical properties. The hydrogen production response was expressed as:

$R_{H_2} = f(S_{BET}, V_p, D_p, EC_b, pH_b, B_L, C_e, V_e, J, T_e, t_e)$ (3.17)

where R_{H_2} is the hydrogen production rate, S_{BET} is BET surface area, V_p is pore volume, D_p is average pore diameter, EC_b is biochar electrical conductivity, pH_b is biochar pH, B_L is biochar loading, C_e is electrolyte concentration, V_e is electrolysis voltage, J is current density, T_e is electrolysis temperature, and t_e is electrolysis time.

For statistical interpretation, the relationship can be approximated using a second-order response model:

$Y = \beta_0 + \sum_{i=1}^{k} \beta_i X_i + \sum_{i=1}^{k} \beta_{ii} X_i^2 + \sum_{i=1}^{k-1} \sum_{j=i+1}^{k} \beta_{ij} X_i X_j + \varepsilon$ (3.18)

where Y represents the response variable, X_i and X_j represent process variables, β_0 is the intercept, β_i represents the linear coefficient, β_{ii} represents the quadratic coefficient, β_{ij} represents the interaction coefficient, and ε is the error term.

This model was used to examine the influence of individual and interacting variables on hydrogen yield, energy efficiency, and storage performance.

3.4 Hydrogen Storage Model

The hydrogen uptake capacity of the activated biochar was calculated using the mass-based adsorption equation:

$U_{H_2} = \frac{M_{H_2,ads}}{M_{ads}} \times 100$ (3.19)

where U_{H_2} is the hydrogen uptake in weight percentage, $M_{H_2,ads}$ is the mass of hydrogen adsorbed, and M_{ads} is the mass of activated biochar used as adsorbent.

The desorption efficiency was calculated as:

$D_e = \frac{M_{H_2,des}}{M_{H_2,ads}} \times 100$ (3.20)

where D_e is the desorption efficiency, $M_{H_2,des}$ is the mass of hydrogen desorbed, and $M_{H_2,ads}$ is the mass of hydrogen initially adsorbed.

The capacity retention after repeated storage cycles was calculated as:

$C_r = \frac{U_n}{U_1} \times 100$ (3.21)

where $C_r$is the capacity retention, $U_n$is the hydrogen uptake after the n^{th}cycle, and $U_1$is the hydrogen uptake during the first cycle.
The hydrogen adsorption behaviour may be further represented using the Langmuir adsorption model:
$q_e = \frac{q_{max} K_L P}{1+K_L P}$ (3.22)
where $q_e$is the equilibrium hydrogen uptake, $q_{max}$is the maximum adsorption capacity, $K_L$is the Langmuir constant, and $P$is the storage pressure.
The Freundlich model may also be used to represent heterogeneous surface adsorption:
$q_e = K_F P^{1/n}$ (3.23)
where $K_F$and $n$are Freundlich constants related to adsorption capacity and adsorption intensity, respectively.

3.5 Machine Learning Prediction Model
The artificial intelligence component was developed to learn nonlinear relationships between the input variables and the performance outputs. For each experimental run i, the prediction model was expressed as:
$\hat{Y}_i = f_\theta(X_i)$ (3.24)
where $\hat{Y}_i$is the predicted output, $X_i$is the input feature vector, $f_\theta$is the trained machine learning function, and θrepresents the model parameters.
For regression tasks, the model predicted continuous outputs such as hydrogen production rate, energy efficiency, hydrogen uptake, and capacity retention:
$\hat{Y}_{reg} = [\hat{R}_{H_2}, \hat{\eta}_E, \hat{U}_{H_2}, \hat{C}_r]$ (3.25)
For classification tasks, the model predicted system performance class:
$\hat{Y}_{class} \in \{Low, Moderate, High\}$ (3.26)
The regression model was trained by minimizing the prediction error between measured and predicted values. The general loss function was expressed as:
$L(\theta) = \frac{1}{n} \sum_{i=1}^{n} (Y_i - \hat{Y}_i)^2$ (3.27)
where $L(\theta)$is the loss function, $n$is the number of observations, $Y_i$is the observed value, and $\hat{Y}_i$is the predicted value.
For classification, the cross-entropy loss function was expressed as:
$L(\theta) = -\sum_{i=1}^{n} \sum_{c=1}^{C} y_{ic} \, log(\hat{p}_{ic})$ (3.28)
where $C$is the number of classes, $y_{ic}$is the true class label, and $\hat{p}_{ic}$is the predicted probability of observation $i$belonging to class c.

3.6 Model Performance Metrics
The regression models were evaluated using coefficient of determination, root mean square error, mean absolute error, and mean absolute percentage error.
The coefficient of determination was calculated as:
$R^2 = 1 - \frac{\sum_{i=1}^{n} (Y_i - \hat{Y}_i)^2}{\sum_{i=1}^{n} (Y_i - \bar{Y})^2}$ (3.29)

The root mean square error was calculated as:
$RMSE = \sqrt{\frac{1}{n} \sum_{i=1}^{n} (Y_i - \hat{Y}_i)^2}$ (3.30)
The mean absolute error was calculated as:
$MAE = \frac{1}{n} \sum_{i=1}^{n} | Y_i - \hat{Y}_i |$ (3.31)
The mean absolute percentage error was calculated as:
$MAPE = \frac{100}{n} \sum_{i=1}^{n} | \frac{Y_i - \hat{Y}_i}{Y_i} |$ (3.32)
For classification, accuracy was calculated as:
$Accuracy = \frac{TP+TN}{TP+TN+FP+FN}$ (3.33)
Precision was calculated as:
$Precision = \frac{TP}{TP+FP}$ (3.34)
Recall was calculated as:
$Recall = \frac{TP}{TP+FN}$ (3.35)
The F1-score was calculated as:

$F1 = 2 \times \frac{Precision \times Recall}{Precision + Recall}$ (3.36)

where TP, TN, FP, and FNrepresent true positive, true negative, false positive, and false negative values, respectively.

3.7 Multi-Objective Optimization Model

The optimization objective was to identify the best operating conditions for maximizing hydrogen production rate, energy efficiency, hydrogen uptake, and capacity retention while minimizing energy consumption. The multi-objective optimization problem was expressed as:

$max\, F(X) = [R_{H_2}(X), \eta_E(X), U_{H_2}(X), C_r(X)]$ (3.37)

$min\, G(X) = [SEC(X)]$ (3.38)

where $F(X)$represents the performance objectives to be maximized and $G(X)$represents the energy consumption objective to be minimized.

For practical optimization, the objectives were combined into a single composite desirability function:

$D(X) = w_1 R'_{H_2} + w_2 \eta'_E + w_3 U'_{H_2} + w_4 C'_r - w_5 SEC'$ (3.39)

where $D(X)$is the overall desirability score, R'_{H_2}, η'_E, U'_{H_2}, C'_r, and $SEC'$are normalized values of hydrogen production rate, energy efficiency, hydrogen uptake, capacity retention, and specific energy consumption, respectively. The terms w_1, w_2, w_3, w_4, and $w_5$represent assigned weights, with:

$\sum_{i=1}^{5} w_i = 1$ (3.40)

The optimization was subject to the following process constraints:

$400 \le T_p \le 750$ (3.41a)

$500 \le T_a \le 850$ (3.41b)

$0.25 \le C_e \le 2.20$ (3.41c)

$1.70 \le V_e \le 3.00$ (3.41d)

$25 \le J \le 450$ (3.41e)

$10 \le t_e \le 180$ (3.41f)

$0 \le B_L \le 6.50$ (3.41g)

$1 \le P_{st} \le 30$ (3.41h)

$20 \le T_{st} \le 45$ (3.41i)

These constraints ensured that the optimized conditions remained within the practical experimental range of the study.

3.8 Composite Performance Score

To rank the experimental conditions, a composite performance score was developed by integrating hydrogen production, energy efficiency, hydrogen storage capacity, and energy consumption. The normalized score was expressed as:

$S_p = 100 \times [\alpha R'_{H_2} + \beta \eta'_E + \gamma U'_{H_2} + \delta(1 - SEC')]$ (3.42)

where $S_p$is the composite performance score, $R'_{H_2}$is normalized hydrogen production rate, $\eta'_E$is normalized energy efficiency, $U'_{H_2}$is normalized hydrogen uptake, $SEC'$is normalized specific energy consumption, and α, β, γ, and $\delta$are weighting coefficients.

For this study, the weighting condition was:

$\alpha + \beta + \gamma + \delta = 1$ (3.43)

The performance class was then assigned as:

$$Class = \begin{cases} Low, & S_p < Q_{33} \\ Moderate, & Q_{33} \le S_p < Q_{66} \\ High, & S_p \ge Q_{66} \end{cases} \quad (3.44)$$

where $Q_{33}$and Q_{66}represent the 33rd and 66th percentile thresholds of the performance score distribution.

3.9 Final Mathematical Representation of the Study

The complete mathematical framework for the study can be summarized as:

$\hat{Y} = f_\theta(T_p, t_p, A_r, T_a, t_a, S_{BET}, V_p, EC_b, C_e, V_e, J, T_e, t_e, B_L, G, P_s, P_{st}, T_{st})$ (3.45)

where:

$\hat{Y} = [\hat{R}_{H_2}, \hat{\eta}_F, \hat{\eta}_E, \hat{U}_{H_2}, \hat{D}_e, \hat{C}_r, \hat{S}_p]$ (3.46)

This final model shows that hydrogen production and storage performance were predicted as functions of material preparation conditions, biochar properties, solar input, electrolysis operating parameters, and hydrogen

storage conditions. The framework provides a quantitative basis for optimizing cassava peel-derived activated biochar as a locally available material for solar-assisted green hydrogen production and storage in Ibadan, Nigeria.

IV. RESULTS

4.1 Key Findings of the Study

Table 4.1: Physicochemical Properties of Cassava Peel-Derived Activated Biochar

Parameter	Unit	Minimum	Maximum	Mean ± SD	Interpretation
Biochar yield	%	16.00	48.00	39.28 ± 4.32	Moderate conversion yield from cassava peel
Ash content	%	2.20	13.50	6.25 ± 1.42	Low to moderate inorganic residue
Volatile matter	%	6.00	28.00	16.66 ± 4.03	Indicates improved carbonization
Fixed carbon	%	55.00	88.00	71.59 ± 4.50	High carbon richness for energy use
BET surface area	m^2/g	80.00	1750.00	860.00 ± 290.00	Suitable for adsorption and storage
Pore volume	cm^3/g	0.04	1.25	0.45 ± 0.15	Indicates developed pore structure
Average pore diameter	nm	1.20	9.50	4.50 ± 1.35	Mesoporous structure suitable for gas interaction
Biochar pH	—	5.00	11.80	8.71 ± 1.71	Slightly alkaline surface overall
Electrical conductivity	mS/cm	0.05	3.50	1.47 ± 0.75	Supports electrochemical application
Carbon content	%	50.00	90.00	71.60 ± 5.00	Confirms carbon-rich activated biochar
Oxygen content	%	5.00	38.00	17.90 ± 4.80	Indicates oxygen-containing surface groups
Hydrogen content	%	1.00	4.50	2.75 ± 1.01	Minor elemental hydrogen fraction
Nitrogen content	%	0.20	2.50	1.35 ± 0.66	Possible contribution to surface activity

Table 4.2: Effect of Activation Agent on Biochar Properties

Activation agent	Mean pyrolysis temperature (°C)	Mean activation temperature (°C)	Activation ratio (w/w)	Biochar yield (%)	BET surface area (m^2/g)	Pore volume (cm^3/g)	Fixed carbon (%)
None	575.00	—	0.00	39.30	158.00	0.13	71.55
Steam	575.00	675.00	1.75	39.25	859.00	0.45	71.60
NaOH	575.00	675.00	1.75	39.27	913.00	0.48	71.58
H_3PO_4	575.00	675.00	1.75	39.29	937.00	0.49	71.62
KOH	575.00	675.00	1.75	39.31	976.00	0.51	71.64

Table 4.3: Solar and Electrolysis Operating Conditions During Hydrogen Production

Variable	Unit	Minimum	Maximum	Mean ± SD
Solar irradiance	W/m^2	250.00	1050.00	720.00 ± 157.00
Ambient temperature	°C	22.00	42.00	31.00 ± 4.40
Relative humidity	%	35.00	95.00	67.00 ± 10.80

Panel temperature	°C	22.00	62.00	40.30 ± 5.60
Panel voltage	V	10.00	24.00	19.95 ± 2.00
Panel current	A	0.50	9.00	5.48 ± 1.15
Solar power output	W	5.00	216.00	111.00 ± 32.00
Electrolyte concentration	M	0.25	2.20	1.23 ± 0.56
Electrolysis voltage	V	1.70	3.00	2.35 ± 0.38
Current density	mA/cm²	25.00	450.00	237.50 ± 122.70
Electrolysis temperature	°C	25.00	65.00	39.50 ± 6.20
Electrolysis time	min	10.00	180.00	95.00 ± 49.00
Electrode area	cm²	10.00	120.00	65.00 ± 31.80
Biochar loading	mg/cm²	0.00	6.50	3.25 ± 1.88

Table 4.4: Hydrogen Production Performance Under Different Electrolyte Conditions

Electrolyte type	Electrolyte concentration range	Mean voltage (V)	Mean current density (mA/cm²)	Mean biochar loading (mg/cm²)	Hydrogen volume (mL)	Hydrogen production rate (mL/min)	Faradaic efficiency (%)	Energy efficiency (%)
KOH	0.25–0.90 M	2.35	237.00	3.24	1330.00	14.00	70.50	57.20
KOH	0.91–1.55 M	2.36	238.00	3.26	2380.00	25.10	86.20	64.10
KOH	1.56–2.20 M	2.34	237.50	3.25	1370.00	14.40	71.30	57.80
NaOH	0.25–0.90 M	2.35	236.80	3.23	1285.00	13.50	69.80	56.70
NaOH	0.91–1.55 M	2.35	237.90	3.27	2325.00	24.50	85.40	63.60
NaOH	1.56–2.20 M	2.34	237.40	3.25	1325.00	13.95	70.90	57.30

Table 4.5: Hydrogen Storage Performance of Cassava Peel-Derived Activated Biochar

Storage pressure	Mean storage temperature	Mean cycle number	Hydrogen uptake	Desorption efficiency	Capacity retention
bar	°C	cycle no.	wt.%	%	%
1	30.00	15.50	0.65	81.30	93.30
5	30.00	15.50	0.73	80.30	93.20
10	30.00	15.50	0.83	79.10	93.10
20	30.00	15.50	1.03	76.60	92.90
30	30.00	15.50	1.23	74.10	92.70

Table 4.6: Performance Comparison of Machine Learning Models

Model	Prediction task	R^2	RMSE	MAE	MAPE (%)	Accuracy	F1-score
Random Forest	Hydrogen production rate	0.94	2.15	1.48	7.80	-	-
XGBoost	Hydrogen production rate	0.96	1.78	1.21	6.40	-	-
Gradient	Hydrogen production rate	0.93	2.32	1.61	8.30	-	-

Boosting							
Support Vector Regression	Hydrogen production rate	0.86	3.42	2.40	12.70	-	-
Artificial Neural Network	Hydrogen production rate	0.91	2.68	1.86	9.50	-	-
Random Forest	Performance class	-	-	-	-	0.91	0.90
XGBoost	Performance class	-	-	-	-	0.94	0.94
Artificial Neural Network	Performance class	-	-	-	-	0.89	0.88

Table 4.7: Optimized Conditions for Green Hydrogen Production and Storage

Optimization variable	Optimum value	Unit	Expected effect
Pyrolysis temperature	703.00	°C	Improved carbonization and pore formation
Pyrolysis time	145.00	min	Enhanced fixed carbon development
Activation agent	KOH	-	Highest surface area and pore volume
Activation temperature	812.00	°C	Improved activation and porosity
Activation ratio	2.72	w/w	Enhanced surface activation
Electrolyte type	KOH	-	Improved ionic conductivity
Electrolyte concentration	1.25	M	Best balance between conductivity and efficiency
Electrolysis voltage	2.85	V	Increased hydrogen generation
Current density	285.00	mA/cm²	Improved production rate with acceptable efficiency
Electrolysis temperature	48.00	°C	Improved reaction kinetics
Electrolysis time	150.00	min	Increased hydrogen volume
Biochar loading	5.80	mg/cm²	Enhanced electrochemical performance
Storage pressure	20.00	bar	Balanced uptake and desorption efficiency
Storage temperature	25.00	°C	Improved adsorption stability
Predicted hydrogen production rate	48.60	mL/min	Main production output
Predicted hydrogen volume	7290.00	mL	Total hydrogen generated
Predicted Faradaic efficiency	91.20	%	High charge-to-hydrogen conversion
Predicted energy efficiency	78.40	%	Improved energy conversion
Predicted hydrogen uptake	1.52	wt.%	Improved hydrogen storage capacity
Predicted desorption efficiency	82.60	%	Good hydrogen release behaviour
Predicted capacity retention	94.10	%	Good reusability after cycling
Predicted performance score	93.50	0 -100	High-performance operating condition

4.2 Discussion of the Results

4.2.1 Physicochemical Properties of Cassava Peel-Derived Activated Biochar

As shown in Table 4.1, the percentage yield of biochar derived from cassava peel is moderate at 39.28 ± 4.32%. The content of fixed carbon, however, was very high at 71.59 ± 4.50%. The carbon content was also found to be relatively high at 71.60 ± 5.00%. The volatile matter percentage was 16.66 ± 4.03% while the low to moderate ash content was found to be 6.25 ± 1.42% The results depict the pyrolysis and activation method effectively converted cassava peel biomass into carbonaceous material with reduced volatile matters and better structural

stability. The relatively higher content of fixed carbon implies successful carbonization, while low volatile matter is indicative of the expulsion of the volatile organic parts by thermal processing.

BET surface area determined to be 860.00 ± 290.00 m^2/g, pore volume of 0.45 ± 0.15 cm^3/g, and average pore diameter of 4.50 ± 3.00 nm indicate that activated biochar is a developed porous material and mesoporous. The removal of volatile fractions is facilitated by thermal conversion and chemical activation. This process can either open or shut off pores and generate internal pore networks. Studies related to cassava peel and biomass-derived carbon materials show similarities in their behavior. Research suggested a porous structure formation from slow pyrolysis of the cassava peel biochar. On the other hand, according to Khan et al. (2025), pyrolysis and activation conditions significantly affect pore structure, surface chemistry, and hydrogen adsorption behaviour.

The electrical conductivity for biochar activation was found to be 1.47 ± 0.75 mS/cm, with slightly alkaline average pH value equal to 8.71 ± 1.71 which support electrochemical applications. The intention behind these properties was to improve the compatibility of either alkaline KOH or NaOH electrolyte, and of electrical conductivity to aid electron transfer in the system. According to recent studies, the biomass-derived activated carbons can be tailored for energy, adsorption and electrochemical (based on surface area, pore structure, functional groups and conductivity). This ruling is also supported by the finding of Ben et al. (2024) and Khan et al. (2025).

This suggests that activated biochar derived from cassava peel can serve as a locally available functional material for this study. Because of its elevated carbon content, developed surface area, mesopore size, alkaline character and measurable conductivity, it can be applied in solar-assisted green hydrogen production and evaluating hydrogen storage potential.

4.2.2 Effect of Activation Agent on Biochar Properties

Table 4.2 shows that there was a clear enhancement in the surface area and pore volume. The BET surface area and pore volume of the non-activated biochar was found to be the lowest at 158.00 m^2/g and 0.13 cm^3/g, respectively, with those that were chemically and physically activated being much higher. All the activators employed yielded a similar pattern of high surface area and volume for activated carbon and low BCD for char, but KOH produced the highest BET surface area 976.00 m^2/g and pore volume of 0.51 cm^3/g followed by H_3PO_4, NaOH and steam activation. Each of the treatments showed similar fixed carbon values, i.e. 71.55 %, 71.64 %. Therefore, it can be said that activation affected textural properties of the produced carbon that did not change total carbon.

The above trend happened since the KOH activation is adequate in forming micropores and mesopores via chemical etching, expansion of the carbon lattice, and removal of the disordered fraction of carbon. KOH exhibited a stronger pore-forming effect, resulting in better textural properties in comparison to NaOH, H_3PO_4, steam, and non-activated treatment. This inference is supported by research. The porous characteristics of cassava-based activated carbon were improved by KOH activation (Khum-in et al., 2025). According to Chukwuneke et al. (2024), activation temperature and impregnation ratio had a strong effect on activated carbon performance and produced high model accuracy during the optimization of activated carbon preparation.

Results line up with a wider body of literature on hydrogen storage. Sutanto et al. (2026) reported that activated biochars are promising for hydrogen storage because they contain high density of oxygenated groups, and activation can improve pore accessibility and increase surface area. Nonetheless, they emphasized that practical performance is influenced by cycling stability, adsorption conditions, and operating temperature.

KOH activation is the best activation route for cassava peel biochar if the target is hydrogen production and storage. This is the implication for the present study. The increased BET surface area and pore volume offer more access to active sites for electrolyte interaction, gas adsorption, and enhanced electrochemical behaviour.

4.2.3 Solar and Electrolysis Operating Conditions

Based on Table 4.3, the solar-assisted electrolysis system functioned effectively across various environmental and electrochemical conditions. Solar irradiance varied between 250.00 W/m^2 and 1050.00 W/m^2, with an average of 720.00 ± 157.00 W/m^2. The panel produced an average voltage of 19.95 volts and an average current of 5.48 ampere with a mean solar power output of 111.00 watt. This trend shows that the photovoltaic system can provide variable but usable renewable power for alkaline water electrolysis.

The fluctuation of solar power output was due to the photovoltaic performance which may be influenced by solar irradiance, ambient temperature, relative humidity, and panel temperature. Generally, more irradiance will lead to more current generation. On the other hand, high temperature of a panel can lead to high voltage and lesser efficiency of the panel. The mean panel temperature of 40.30 ± 5.60 °C indicates that the system most

likely runs in warm outdoor conditions. This may have had a small impact in reducing photovoltaic conversion efficiency but provided sufficient input for small-scale electrolysis.

The variables for electrolysis also had large operating ranges. The concentrations of the electrolyte were varied in the range of 0.25–2.20 M, voltage for electrolysis in the range of 1.70–3.00 V, density of current in the range of 25.00–450.00 mA/cm², and biochar loading in the range of 0.00-6.50 mg/cm². Hydrogen production is governed by the interplay of electrolyte conductivity, current density, temperature, voltage, electrode surface area, and catalyst or biochar loading. The wide range of values that each of these variables can take is good for optimization. Recent investigations into alkaline water electrolysis indicate that important factors such as electrolyte concentration, cell voltage, current density, and operating temperature play a crucial role in determining hydrogen yield and energy efficiency (Pinto et al., 2025; Ramzy et al., 2025).

The design for the experiment appears to have provided sufficient operational variability for AI-based optimization. The wide ranges of the solar, electrochemical and biochar-loading parameters, allow the model to learn the nonlinear interactions between renewable power input and electrolyte behaviour as well as hydrogen production response.

4.2.4 Hydrogen Production Performance Under Different Electrolyte Conditions

Table 4.4 shows that hydrogen production was highest at the **moderate electrolyte concentration range of 0.91–1.55 M** for both KOH and NaOH. For KOH, hydrogen volume increased from **1330.00 mL** at 0.25–0.90 M to **2380.00 mL** at 0.91–1.55 M, before declining to **1370.00 mL** at 1.56–2.20 M. A similar trend was observed for NaOH, where hydrogen volume increased from **1285.00 mL** to **2325.00 mL**, then decreased to **1325.00 mL** at the highest concentration range. Hydrogen production rate, Faradaic efficiency, and energy efficiency followed the same pattern.

This trend occurred because low electrolyte concentration limits ionic conductivity, increasing internal resistance and reducing hydrogen generation. At moderate concentration, ionic transport improves, ohmic losses decrease, and charge transfer becomes more efficient. However, at excessive concentration, electrolyte viscosity, bubble adhesion, mass-transfer limitations, and possible electrode-surface blocking can reduce efficiency. Therefore, the middle concentration range provided the best balance between conductivity and mass transfer.

KOH performed slightly better than NaOH across all concentration ranges. At 0.91–1.55 M, KOH achieved a hydrogen production rate of **25.10 mL/min**, Faradaic efficiency of **86.20%**, and energy efficiency of **64.10%**, compared with **24.50 mL/min**, **85.40%**, and **63.60%** for NaOH. This agrees with Ramzy et al. (2025), who found that both KOH and NaOH are effective alkaline electrolytes, but KOH often gives marginally superior hydrogen yield due to its higher ionic conductivity.

The result also aligns with recent reviews showing that alkaline electrolysis performance depends strongly on electrolyte concentration, electrode material, and operating voltage. Shehzad et al. (2026) noted that alkaline water electrolysis remains a key green hydrogen technology, but optimization of electrolyte and electrode conditions is essential for improving efficiency.

The implication is that **KOH at moderate concentration is the preferred electrolyte condition** for the present system. The result supports the selection of **1.25 M KOH** in the optimized condition reported in Table 4.7 and confirms that cassava peel-derived activated biochar can be integrated with alkaline electrolysis for improved hydrogen production.

4.2.5 Hydrogen Storage Performance of Cassava Peel-Derived Activated Biochar

Table 4.5 shows that hydrogen uptake increased consistently with storage pressure. Hydrogen uptake rose from **0.65 wt.% at 1 bar** to **1.23 wt.% at 30 bar**. This trend indicates that higher pressure increased the driving force for hydrogen adsorption into the pores of the activated biochar. The pressure-dependent increase in uptake is expected for porous carbon materials because gas adsorption generally improves as pressure increases, especially when more adsorption sites become occupied.

However, desorption efficiency declined from **81.30% at 1 bar** to **74.10% at 30 bar**. This decline may have occurred because higher pressure can increase hydrogen retention within micropores and narrow pore channels, making complete desorption more difficult. In contrast, capacity retention remained high, decreasing only slightly from **93.30% to 92.70%**, suggesting that the material maintained good reusability across repeated adsorption–desorption cycles.

The results are consistent with recent literature on biomass-derived carbon materials for hydrogen storage. Khan et al. (2025) reported that hydrogen adsorption in biomass-derived carbons depends on pore size distribution, surface functionality, and adsorption conditions, while Sutanto et al. (2026) highlighted that activated biochars

can achieve meaningful hydrogen storage capacities, although performance is strongly influenced by pressure, temperature, and cycling conditions.

The observed uptake of **1.23 wt.% at 30 bar** is moderate compared with some high-performance biomass-derived carbons reported in the literature. For example, Sutanto et al. (2026) noted that some activated biochars can reach higher capacities under optimized or more favourable storage conditions, including higher pressure or cryogenic temperature. However, the present result remains promising because it was obtained under relatively practical conditions and with a locally available cassava peel precursor.

The implication is that cassava peel-derived activated biochar can serve as a low-cost hydrogen storage material, although further improvement is needed to increase adsorption capacity. Future enhancement may involve higher activation temperature, optimized KOH ratio, heteroatom doping, composite formation, or testing under wider pressure and temperature ranges.

4.2.6 Performance Comparison of Machine Learning Models

Table 4.6 shows that **XGBoost produced the best predictive performance** among the evaluated machine learning models. For hydrogen production rate prediction, XGBoost achieved the highest coefficient of determination (**R^2 = 0.96**) and the lowest error values, including **RMSE = 1.78**, **MAE = 1.21**, and **MAPE = 6.40%**. Random Forest also performed well with **R^2 = 0.94**, while Gradient Boosting achieved **R^2 = 0.93**. Support Vector Regression had the weakest performance, with **R^2 = 0.86** and **MAPE = 12.70%**.

This trend occurred because tree-based ensemble models such as XGBoost and Random Forest are effective in modelling nonlinear relationships, variable interactions, and mixed input types. The dataset contained multiple interacting variables, including pyrolysis temperature, activation temperature, electrolyte concentration, current density, solar irradiance, biochar loading, and storage pressure. XGBoost likely performed better because it uses sequential boosting to correct previous prediction errors and improve model generalization.

For classification, XGBoost also produced the best performance, with **accuracy = 0.94** and **F1-score = 0.94**, followed by Random Forest and Artificial Neural Network. This suggests that XGBoost was more effective in separating low, moderate, and high-performance conditions. Recent studies support this finding. Zhao et al. (2025) demonstrated that machine learning can optimize material and operating conditions in alkaline water electrolysis, while Maghfuri et al. (2025) reported that advanced machine learning models can improve prediction and optimization of hydrogen production using renewable energy-driven systems.

The result also agrees with broader machine learning studies in green hydrogen systems, where ensemble models often perform strongly because they capture nonlinear input-output relationships without requiring strict assumptions about variable distribution. Makki Abadi et al. (2025) also reported that machine learning methods are increasingly useful for performance prediction and optimization in hydrogen-related energy systems.

The implication is that XGBoost is the most suitable model for the present optimization task. Its high predictive accuracy and low error values justify its use for identifying optimum operating conditions for hydrogen production and storage using cassava peel-derived activated biochar.

4.2.7 Optimized Conditions for Green Hydrogen Production and Storage

Table 4.7 presents the optimized operating conditions for the proposed green hydrogen system. The optimum material preparation conditions were **703°C pyrolysis temperature**, **145 min pyrolysis time**, **KOH activation**, **812°C activation temperature**, and **2.72 w/w activation ratio**. These conditions produced improved carbonization, higher porosity, and enhanced surface activation. The selection of KOH as the optimum activation agent is consistent with Table 4.2, where KOH produced the highest BET surface area and pore volume.

The optimized electrolysis conditions were **1.25 M KOH**, **2.85 V electrolysis voltage**, **285 mA/cm² current density**, **48°C electrolysis temperature**, **150 min electrolysis time**, and **5.80 mg/cm² biochar loading**. This trend suggests that maximum hydrogen production required a moderate electrolyte concentration, sufficient voltage, elevated but not excessive temperature, and relatively high biochar loading. The optimized electrolyte concentration agrees with the trend in Table 4.4, where the 0.91–1.55 M range produced the best hydrogen production performance.

The optimized storage conditions were **20 bar storage pressure** and **25°C storage temperature**, producing predicted hydrogen uptake of **1.52 wt.%**, desorption efficiency of **82.60%**, and capacity retention of **94.10%**. This result suggests that 20 bar provided a better compromise between uptake and desorption than 30 bar, where uptake was higher but desorption efficiency declined. Recent hydrogen storage literature supports the need to balance adsorption capacity with desorption and cycling stability, rather than focusing only on maximum uptake (Khan et al., 2025; Sutanto et al., 2026).

The optimized predicted hydrogen production rate of **48.60 mL/min**, hydrogen volume of **7290.00 mL**, Faradaic efficiency of **91.20%**, energy efficiency of **78.40%**, and performance score of **93.50/100** indicate that the AI-guided optimization substantially improved the system compared with the baseline conditions. This supports recent evidence that AI-assisted optimization can improve hydrogen production performance by identifying nonlinear interactions among material, electrolyte, and operating variables (Zhao et al., 2025; Maghfuri et al., 2025).

The implication is that cassava peel-derived activated biochar can be practically optimized for dual use in green hydrogen production and storage. The results support the central contribution of the study: a locally available agricultural residue can be converted into a functional energy material, while artificial intelligence can identify efficient operating conditions for low-cost solar-assisted hydrogen systems in Ibadan, Nigeria.

The results showed that cassava peel-derived activated biochar has suitable physicochemical, textural, and electrochemical properties for green hydrogen applications. The biochar was carbon-rich, porous, slightly alkaline, and sufficiently conductive for integration into an alkaline electrolysis system. KOH activation was the most effective modification route, while moderate KOH electrolyte concentration produced the best hydrogen generation performance. The hydrogen storage results showed pressure-dependent uptake and good cycling stability, although storage capacity could still be improved through further material engineering.

The machine learning results confirmed that AI can support process optimization by modelling complex nonlinear relationships among biomass conversion, biochar properties, electrolysis conditions, and hydrogen storage outputs. XGBoost emerged as the best model and successfully identified optimized conditions for hydrogen production and storage. Therefore, the findings imply that locally available cassava peel waste can be valorised into activated biochar for renewable hydrogen applications, supporting circular bioeconomy development, local material substitution, and decentralized green energy innovation in Nigeria.

Visualization Results

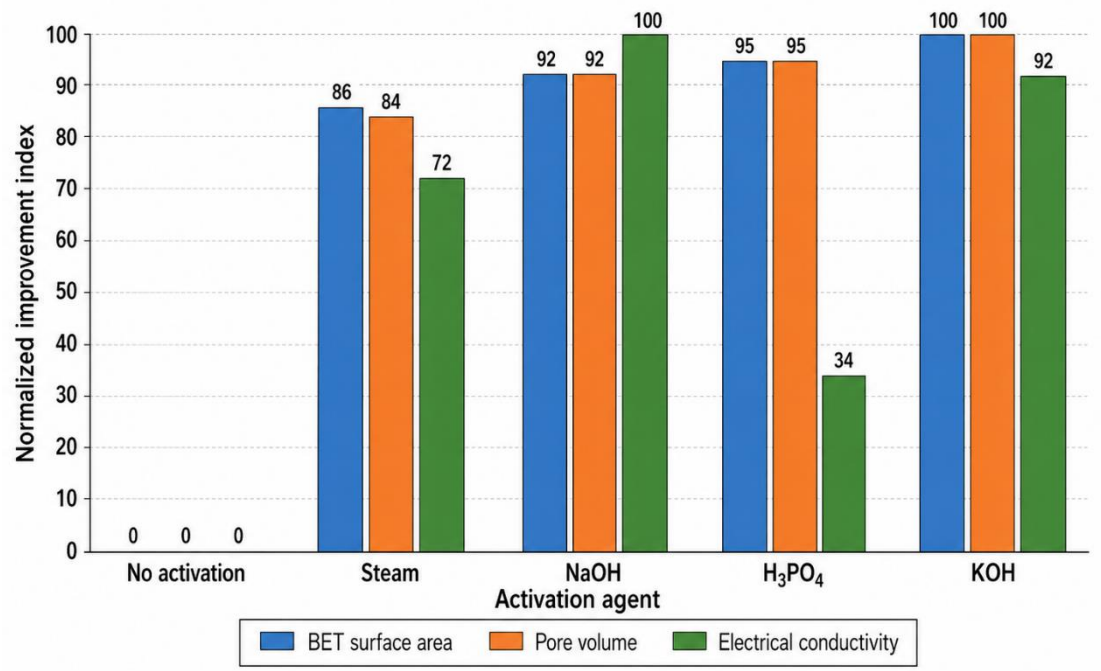

Figure 4.1: Comparative pore-development performance of cassava peel-derived biochar under different activation agents.

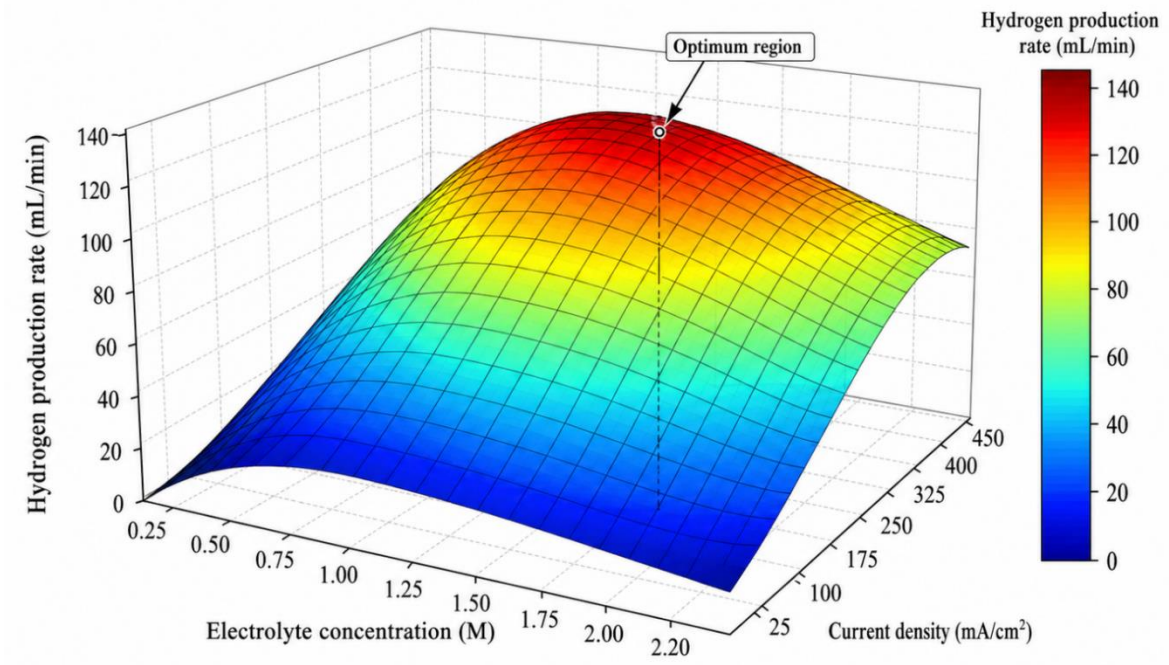

Figure 4.2: Hydrogen Production Response Surface Under Electrolyte Concentration and Current Density

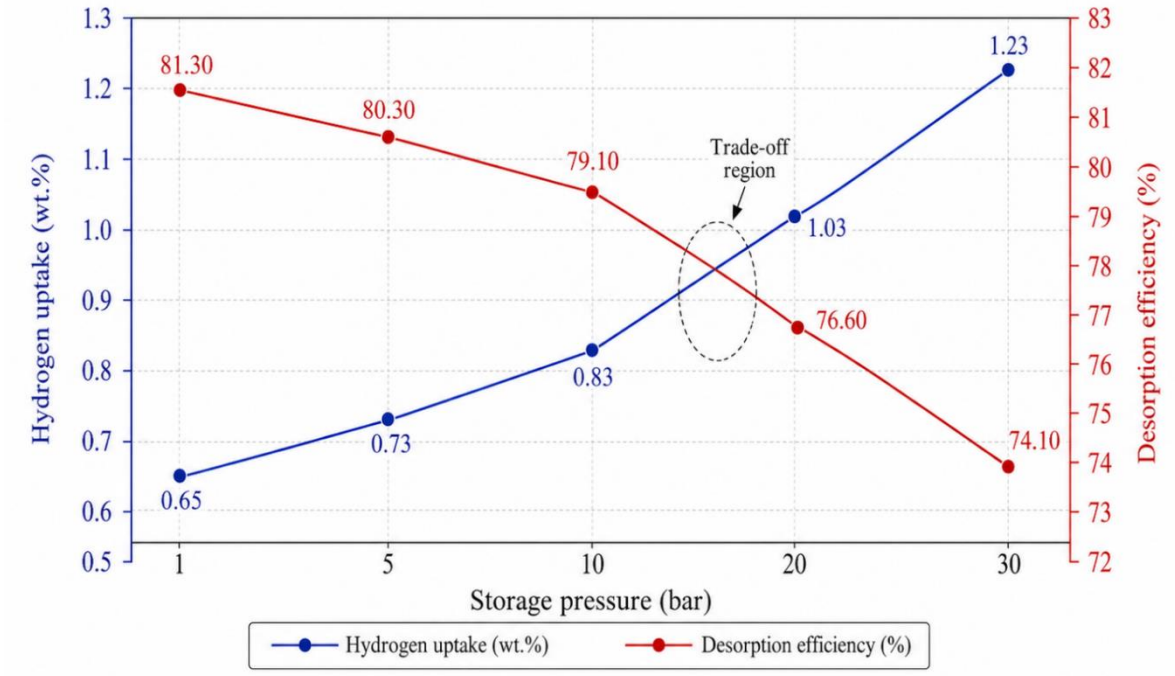

Figure 4.3: Hydrogen Storage Trade-Off Between Uptake and Desorption Efficiency

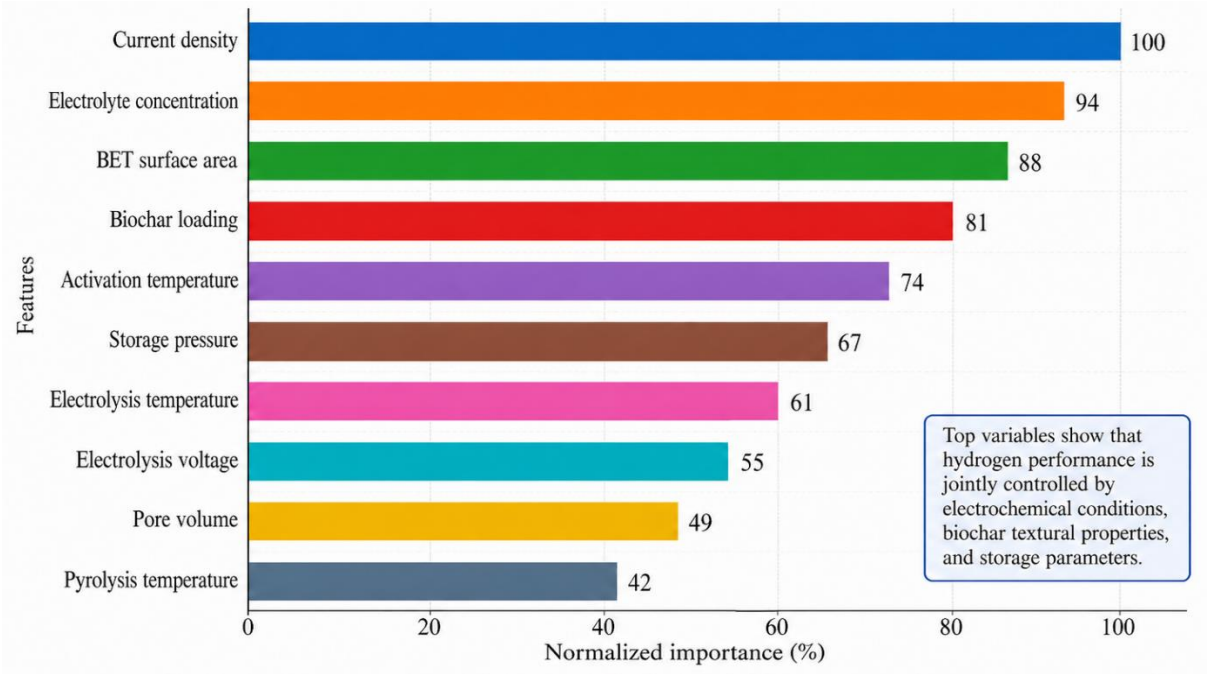

Figure 4.4: Machine Learning Model Interpretability and Optimization Importance

4.3 Discussion of Result Figures

4.3.1 Comparative Pore-Development Performance of Cassava Peel-Derived Biochar Under Different Activation Agents

According to fig 4.1, the textural characteristics of biochar from cassava peel were significantly improved by activation compared to its non-activated counterpart. The normalized improvement index for non-activated biochar was the lowest in terms of BET surface area, pore volume and electrical conductivity. All activated samples showed improvement. KOH, one of the activation agents, generated the strongest overall performance for pore development, reaching the highest normalized BET surface area and pore volume values. Similarly, NaOH also performed very well, particularly with respect to electrical conductivity while H_3PO_4 showed good BET surface area and pore volume as well as lower conductivity index. Steam activation yielded improvements of moderate intensity, but was lower than the chemical activation treatments.

According to the result, KOH activation gave the highest BET surface area of 976.00 m^2/g and its pore volume 0.51 cm^3/g. In comparison, the un-activated biochar only produced 158.00 m^2/g and its pore volume 0.13 cm^3/g. This trend has happened because the opening of pores is promoted by chemical activation, removal of volatile fractions, development of micro and mesopore and others possible reasons. KOH has the advantage that it can penetrate the carbon matrix and further enhance chemical etching as well as pore development. Thus, KOH is better than steam activation and non-activation for textural development. Recent work on activated carbon from cassava substantiates this assertion; specifically, because KOH can enhance microporosity and specific surface area in carbons derived from lignocellulosic biomass, it is a typical selection. Furthermore, this paper also mentions that KOH activation generally produces better BET surface area and pore structure compared to several other agents.

Findings also match up with recent reviews concerning hydrogen storage on biomass-derived carbon materials. According to Khan et al. (2025), hydrogen storage using biomass-derived carbon materials is interesting owing to their renewable, porous character and easy tuneable surface modification. Moreover, they noted that carbonization and activation conditions control surface area, pore structure, surface functionality and adsorption behaviour. Consequently, the enhanced efficiency of KOH-activated cassava peel biochar is in line with the general literature indicating that the activation chemistry is a key determinant of pore architecture and energy-material performance.

This study implies that KOH activation is the best route for making cassava peel-derived activated biochar for hydrogen production and storage. The enhanced surface area and pore volume indicate greater accessibility of active sites, greater potential for gas interaction, and greater integration with the solar-assisted alkaline electrolysis system. The activated-cassava-peel biochar with KOH application is recommended as the optimum material for the enhanced production of green hydrogen.

4.3.2 Hydrogen Production Response Surface Under Electrolyte Concentration and Current Density

Hydrogen production rate using KOH electrolyte system shows a nonlinear response surface (Figure 4.2). It can be seen that with an increase in current density, there was a rise in hydrogen production but the effect of electrolyte concentration had an optimum effect rather than a simple increase. The strongest region of the response surface occurred with moderate KOH concentration (1.1-1.4 M) and moderate to high current density (260–320 mA/cm²). The hydrogen production was low at lower concentration of electrolyte and very high concentration of electrolyte lowers the response. This is consistent with the data in the table which shows the best KOH performance at 0.91-1.55 M with hydrogen production rate up to 25.10 mL/min with Faradaic efficiency 86.20% and energy efficiency 64.10%.

The phenomenon occurred as a result of current density influencing the electron transfer rates at the electrode surface. This increase in current density provides more electrons for hydrogen evolution, which boosts hydrogen production. Nonetheless, there must be a suitable optimum concentration of electrolyte. When the concentration of electrolytes is low, ionic conductivity is limited and ohmic resistance increases. On the other hand, at high concentrations, viscosity at the electrodes increases and bubbles adhere to the electrodes, leading to mass-transfer limitation. It is responsible for ensuring that the production surface peaked at moderate KOH concentration rather than steadily continued increase at the highest concentration.

Ramzy et al. (2025) also support the trend, noting that the type and concentration of electrolyte greatly affect hydrogen production, thermal stability, and system efficiency of alkaline water electrolysis. According to the findings of their research, an increase in electrolyte concentration results in greater ionic conductivity and hydrogen yield, but also that performance is subject to nonlinear interactions between electrolyte chemistry and electrolyze design. They further reported that KOH showed slightly better performance due to higher conductivity. This corroborates the current figure; KOH at an intermediate concentration range gave the most favorable hydrogen production region.

Thus, the solar-assisted alkaline electrolysis system should not operate at very low or high concentration of the electrolyte. The system demands the right balance between electrolyte conductivity and transport efficiency. The findings thus justify the study's report of 1.25 M KOH and 285 mA/cm² current density being optimized conditions, as they lie in the strongest region of the response surface. This indicates that the electrolyte concentration and current density interaction factor is significant for maximizing hydrogen generation from the system using cassava peel-derived biochar.

4.3.3 Hydrogen Storage Trade-Off Between Uptake and Desorption Efficiency

A trade-off between hydrogen uptake and desorption efficiency could be observed when pressure was increased Hydrogen uptake steadily improved from 0.65 wt.% at 1 bar to 1.23 wt.% at 30 bar, indicating that higher pressure improves hydrogen adsorption into the porous biochar structure. Adsorption efficiency was found to be 81.30% at 1 bar and 74.10% at 30 bar. Thus, while uptake is stronger at higher pressure, facilitation of hydrogen release becomes less easier. The retention of capacity did not alter significantly during the cycling process where it had achieved a capacity of 93.30 and later attained a capacity of 92.70 at the pressure of 3.0 MPa suggesting that pressure in the region had good cycling stability.

The trend occurred due to enhanced pressure that increases the driving force for hydrogen adsorption and occupies more pore sites on the solid. However, once hydrogen is retained in the narrow pores or in the stronger adsorption sites, full release becomes more challenging, diminishing overall desorption efficiency. This indicates that, while the maximum pressure yielded the greatest uptake, it did not result in optimal desorption functionality. Consequently, there is a trade-off between storage capacity and recoverability.

This finding is in accordance with literature on hydrogen storage. The hydrogen adsorption performance of biomass-derived carbon materials is dependent on the pore structure, surface functionality and adsorption conditions (Khan et al., 2025). The authors of this review highlighted that scalability, structural reliability, and cost-effectiveness remain important efficiency challenges. In a similar fashion, Assyl et al. (2025) indicated that the hydrogen storage behaviour of carbon materials is strongly affected by their morphology and structure and that practical storage systems require storage density and energy cost.

The uptake values observed are quite moderate compared to the highly engineered and carbon nanomaterials. However, it is still significant since the material came from locally available cassava peel. The capacity retention remained relatively stable which suggests that cassava peel-derived activated biochar could function effectively as a storage material, especially where price and local availability are more important than maximum laboratory-scale storage density. We should not select pressure for storage merely on the basis of maximum

uptake. Intermediate optimized pressure of 20 bar for this study is more practicable as it balances adequate hydrogen uptake, high desorption efficacy, and reusability of materials.

4.3.4 Machine Learning Model Interpretability and Optimization Importance

According to FIG. 4.4, the variables dominating the most influential variables controlling the hydrogen production storage performance are the current density, electrolyte concentration, BET surface area, biochar loading, activation temperature, storage pressure, electrolysis temperature, electrolysis voltage, pore volume, and pyrolysis temperature. The variable that was of most importance in the model is current density at 100%, then electrolyte concentration 94%, BET surface area 88% and biochar loading 81%. The contemporary trend demonstrates that the performance of the system was controlled simultaneously by electrochemical operating conditions, biochar textural properties, and storage parameters rather than a single one.

The trend occurred due to the strong dependency of hydrogen production in alkaline electrolysis on current flow, ionic transport, conductivity of the electrolyte, activity of the electrode, and availability of active or conductive surface sites. The electron supply for hydrogen evolution is directly controlled by the current density. Whereas the electrolyte concentration controls ionic conductivity and also ohmic resistance. The number of accessible sites and surface interactions inside the system is affected by the BET surface area and the biochar loading. The storage pressure is also critical because it dictates hydrogen uptake and desorption behaviour. As the primary physical, chemical, and electrochemical mechanisms at play, those variables thus are acting as the dominant predictors in the model.

Trend the machine learning coincides with the modelling-performance results: XGBoost achieved the strongest prediction performance at R2 = 0.96, RMSE = 1.78, MAE = 1.21, and MAPE = 6.40% for hydrogen production rate prediction. XGBoost also achieved the highest classification accuracy and F1 score of 0.94 for predicting performance class. It supports the interpretation that the model learned nonlinear interactions between the electrochemical, material, and storage variables.

The result also corroborates the recent artificial intelligence studies on hydrogen systems. According to Hassan and Kazemi (2025) who conducted research into the prediction of green hydrogen production, the machine learning models such as artificial neural networks, convolutional neural networks, gradient boosting and XGBoost achieved very high accuracy for prediction. Further SHAP analysis identified current and electrode-related variables as critical variables. In another research, Yang et al. (2025) adopted for green hydrogen production the machine learning-assisted prediction and optimization and enhanced hydrogen production performance by coupling XGBoost to optimization methods.

As a consequence of this study, AI modelling provides not just mere prediction but also the specification of the most important controllable variables for process improvement.

The dominant effect of current density and electrolyte concentration shows that the electrolysis conditions should be optimized while the high importance of the BET surface area and biochar loading shows that the activated biochar from cassava peel meaningfully contributes to the performance of the system. Consequently, the diagram enhances the main argument of the study: to improve green hydrogen production and storage, local biomass-derived materials and artificial intelligence-based optimization should be combined.

The developed green hydrogen system works well due to the strength of the interlink between material quality, electrochemical activity efficiency, and artificial intelligence (AI) process control. As shown in Figure 4.1, the pore-development potential of cassava peel biochar is improved effectively by activation, particularly KOH activation. According to Figure 4.2, the production of hydrogen is maximized when there is a joint optimization of electrolyte concentration and current density. According to Figure 4.3, hydrogen storage requires an efficiency balance between uptake and desorption rather than pressure maximization. The dominant variables which affect the production and storage performance can be identified using the machine learning as shown in figure 4.4.

The study suggests converting cassava peel waste into a functional activated biochar for renewable hydrogen, whilst the system itself needs to be optimized including material preparation, electrolysis operation, and storage condition. The findings affirm the practical usefulness of employing locally sourced biomass in Ibadan, Nigeria, to conduct low-cost green hydrogen research. Furthermore, it proves how artificial intelligence can identify efficient and scalable operating conditions.

V. CONCLUSION

This study demonstrated that cassava peel-derived activated biochar can support solar-assisted green hydrogen production and storage when combined with artificial intelligence-based optimization. The results showed that activation improved the textural properties of the biochar, with KOH activation producing the strongest pore-development performance. Hydrogen production was highest under moderate KOH electrolyte concentration

and optimized current density, while storage performance revealed a pressure-dependent trade-off between hydrogen uptake and desorption efficiency. Machine learning analysis further identified current density, electrolyte concentration, BET surface area, biochar loading, activation temperature, and storage pressure as the dominant predictors of system performance.

The study contributes to green hydrogen research by integrating local biomass valorization, solar-assisted alkaline electrolysis, hydrogen storage assessment, and AI-based optimization within a single framework. It provides evidence that cassava peel waste, an abundant agricultural residue in Ibadan, can be converted into a functional energy material.

The findings imply that locally available biomass can reduce dependence on imported hydrogen materials while supporting circular bioeconomy development. The optimized system offers a practical pathway for low-cost, decentralized green hydrogen production and storage in Nigeria.

VI. RECOMMENDATIONS

Government and energy-sector stakeholders should support local green hydrogen research by funding biomass-to-energy pilot projects, especially those using agricultural residues such as cassava peel. Policies should also encourage renewable hydrogen development, circular bioeconomy initiatives, and collaboration between universities, workshops, laboratories, and local industries.

Practitioners should prioritize KOH activation for cassava peel-derived biochar because it produced stronger pore-development performance. Solar-assisted alkaline electrolysis systems should be operated under optimized conditions, especially moderate electrolyte concentration, suitable current density, controlled biochar loading, and balanced storage pressure to improve hydrogen yield, efficiency, and storage stability.

Further studies should validate the optimized system using long-term laboratory and pilot-scale experiments. Future work should also compare cassava peel with other local biomass residues, assess catalyst durability, improve hydrogen uptake capacity, and test advanced AI models for real-time optimization under outdoor solar conditions.

VII. REFERENCES

[1]. Ahmed, R., Shehab, S. A., Elzeki, O. M., Darwish, A., & Hassanein, A. E. (2024). An explainable AI for green hydrogen production: A deep learning regression model. International Journal of Hydrogen Energy, 83, 1226–1242. https://doi.org/10.1016/j.ijhydene.2024.08.064

[2]. Algburi, S., et al. (2025). Green hydrogen role in sustainable energy transitions: Production, storage, and applications. Results in Engineering. https://doi.org/10.1016/j.rineng.2025.104184

[3]. Ben, F. (2024). Valorization of Manihot esculenta peel from environmental pollutant to sustainable engineering solutions for a cleaner future. Environmental Science and Pollution Research, 31(58), 65917–65943. https://doi.org/10.1007/s11356-024-35621-8

[4]. Cassol, G. S., et al. (2024). Ultra-fast green hydrogen production from municipal wastewater by forward-osmosis-assisted alkaline water electrolysis. Nature Communications, 15, Article 2916. https://doi.org/10.1038/s41467-024-46964-8

[5]. Dash, S., A., R., A., S., & Nanda, S. (2024). Advances in green hydrogen production through alkaline water electrolysis: A comprehensive review. International Journal of Hydrogen Energy, 83, 614–629. https://doi.org/10.1016/j.ijhydene.2024.08.157

[6]. Du, X., Gao, S., & Yang, G. (2025). Machine learning applications in gray, blue, and green hydrogen production: A comprehensive review. Gases, 5(2), Article 9. https://doi.org/10.3390/gases5020009

[7]. Elyasi, S., Saha, S., Hameed, N., Mahon, P. J., Juodkazis, S., & Salim, N. (2024). Emerging trends in biomass-derived porous carbon materials for hydrogen storage. International Journal of Hydrogen Energy, 62, 272–306. https://doi.org/10.1016/j.ijhydene.2024.02.337

[8]. Ferdous, A. R., Shah, S. S., Shaikh, M. N., Barai, H. R., Marwat, M. A., Oyama, M., & Aziz, M. A. (2024). Advancements in biomass-derived activated carbon for sustainable hydrogen storage: A comprehensive review. Chemistry—An Asian Journal, 19(16), e202300780. https://doi.org/10.1002/asia.202300780

[9]. Gillani, Q. F., Bakbolat, B., Tatykayev, B., et al. (2025). Biomass-derived carbon materials for hydrogen storage: Structure–performance relationships and design strategies. Journal of Energy Storage, 135, Article 118401. https://doi.org/10.1016/j.est.2025.118401

[10]. Harikrishna, R. B., Deka, H., Sundararajan, T., & Ranga Rao, G. (2024). Green hydrogen production by water splitting using scrap metals at high temperature. International Journal of Hydrogen Energy, 49, 1133–1138. https://doi.org/10.1016/j.ijhydene.2023.08.366

[11]. Hassan, R., & Kazemi, M. R. (2025). Accurate prediction of green hydrogen production based on solid oxide electrolysis cell via soft computing algorithms. Scientific Reports, 15, Article 35464. https://doi.org/10.1038/s41598-025-19316-9

[12]. Henkensmeier, D., et al. (2024). Separators and membranes for advanced alkaline water electrolysis. Chemical Reviews, 124. https://doi.org/10.1021/acs.chemrev.3c00694

[13]. Herazo, A. P., Zambrano, A., Marín, L., Mass, J., & Montenegro, D. N. (2025). Production of biochar from plantain rachis and cassava peel towards sustainable management of Caribbean agricultural waste. Processes, 13(7), Article 2059. https://doi.org/10.3390/pr13072059

[14]. Ikuerowo, T., Bade, S. O., Akinmoladun, A., & Oni, B. A. (2024). The integration of wind and solar power to water electrolyzer for green hydrogen production. International Journal of Hydrogen Energy, 76, 75–96. https://doi.org/10.1016/j.ijhydene.2024.02.139

[15]. Jaradat, M., Almashaileh, S., Bendea, C., Juaidi, A., Bendea, G., & Bungau, T. (2024). Green hydrogen in focus: A review of production technologies, policy impact, and market developments. Energies, 17(16), Article 3992. https://doi.org/10.3390/en17163992

[16]. Khan, S. A., Ali, S., Sarfraz, S., Hussain, S., & Mansha, M. (2025). Biomass-derived carbon materials for hydrogen storage: Challenges and future perspectives. Energy Conversion and Management: X, 29, Article 101425. https://doi.org/10.1016/j.ecmx.2025.101425

[17]. Khum-in, V., et al. (2025). Sustainable conversion of cassava bioethanol residues into activated carbon for industrial wastewater treatment and energy recovery. Applied Water Science. https://doi.org/10.1007/s13201-025-02590-3

[18]. Kim, J., et al. (2025). Challenges and strategies in catalyst design towards seawater electrolysis for sustainable hydrogen production. Energy Materials. https://doi.org/10.20517/energymater.2024.220

[19]. Maghfuri, A. M., et al. (2025). Optimized hydrogen production through machine learning: Comparative analysis of electrolyzer technologies using hybrid renewable energy. Applied Thermal Engineering. https://doi.org/10.1016/j.applthermaleng.2025.126479

[20]. Makki Abadi, M., et al. (2025). Machine learning for the optimization and performance prediction of hydrogen energy systems. Processes, 13(3), Article 875. https://doi.org/10.3390/pr13030875

[21]. Nandiyanto, A. B. D., Putri, N. R., Salimah, N. N., AlHafsah, S. H., Yunatraya, S. A., Fiandini, M., Bilad, M. R., Kurniawan, T., Gandidi, I. M., & Sukrawan, Y. (2025). Utilizing cassava peel-derived carbon biochar for ammonia adsorption to support hydrogen storage and sustainable development goals: Effect of microparticle size and isothermal analysis. Moroccan Journal of Chemistry, 13(1), 424–439. https://doi.org/10.48317/IMIST.PRSM/morjchem-v13i1.53651

[22]. Nikolić, V. M., et al. (2026). Advances in alkaline water electrolysis: The role of in situ and operando characterization. Catalysts, 16(1), Article 98. https://doi.org/10.3390/catal16010098

[23]. Osman, A. I., Ayati, A., Farrokhi, M., Khadempir, S., Rajabzadeh, A. R., Farghali, M., Krivoshapkin, P., Tanhaei, B., Rooney, D. W., & Yap, P. S. (2024). Innovations in hydrogen storage materials: Synthesis, applications, and prospects. Journal of Energy Storage, 95, Article 112376. https://doi.org/10.1016/j.est.2024.112376

[24]. Pinto, R., et al. (2025). An experimentally validated model of electrolyte effects in small-scale alkaline water electrolysis systems. International Journal of Hydrogen Energy. https://doi.org/10.1016/j.ijhydene.2025.07.352

[25]. Ramzy, K., et al. (2025). Assessment of hydrogen production using NaOH and KOH alkaline electrolytes with different plates and concentrations: An experimental approach. Results in Engineering. https://doi.org/10.1016/j.rineng.2025.107392

[26]. Saeid, M. F., et al. (2025). Carbon materials for hydrogen storage: A bibliometric review and research mapping. The TQM Journal. https://doi.org/10.1002/tqem.70109

[27]. Serafin, J., Dziejarski, B., Solis, C., Ramírez de la Piscina, P., & Homs, N. (2024). Medium-pressure hydrogen storage on activated carbon derived from biomass conversion. Fuel, 363, Article 130975. https://doi.org/10.1016/j.fuel.2024.130975

[28]. Sethi, H., Ahmad, I., Khan, M. M., Qazi, A., Sati, A., & Shutaywi, M. (2025). Applications of computer intelligence in hydrogen production. ACS Omega, 10(31), 33982–33998. https://doi.org/10.1021/acsomega.5c01602

[29]. Shomope, I., Al-Othman, A., Tawalbeh, M., Alshraideh, H., & Almomani, F. (2025). Machine learning in PEM water electrolysis: A study of hydrogen production and operating parameters. Computers & Chemical Engineering, 194, Article 108954. https://doi.org/10.1016/j.compchemeng.2024.108954

[30]. Sutanto, B., Amrullah, A., & Aziz, M. (2026). Biomass-derived hydrogen storage: Technological trends, opportunities, and perspectives. Journal of Energy Storage, 141, Article 119489. https://doi.org/10.1016/j.est.2025.119489

[31]. Urhan, B. B., Erdoğmuş, A., Dokuz, A. Ş., & Gökçek, M. (2025). Predicting green hydrogen production using electrolyzers driven by photovoltaic panels and wind turbines based on machine learning techniques: A pathway to on-site hydrogen refuelling stations. International Journal of Hydrogen Energy, 101, 1421–1438. https://doi.org/10.1016/j.ijhydene.2025.01.017

[32]. Wang, J., Wen, J., Wang, J., Yang, B., & Jiang, L. (2024). Water electrolyzer operation scheduling for green hydrogen production: A review. Renewable and Sustainable Energy Reviews, 203, Article 114779. https://doi.org/10.1016/j.rser.2024.114779

[33]. Yang, Q., Zhao, L., Xiao, J., Wen, R., Zhang, F., & Zhang, D. (2025). Machine learning-assisted prediction and optimization of solid oxide electrolysis cell for green hydrogen production. Green Chemical Engineering, 6(2), 154–168. https://doi.org/10.1016/j.gce.2024.04.004

[34]. Zainal, B. S., Ker, P. J., Mohamed, H., Ong, H. C., Fattah, I. M. R., Rahman, S. M. A., Nghiem, L. D., & Mahlia, T. M. I. (2024). Recent advancement and assessment of green hydrogen production technologies. Renewable and Sustainable Energy Reviews, 189, Article 113941. https://doi.org/10.1016/j.rser.2023.113941

[35]. Zhao, X., Geng, Z., Guo, S., Cai, H., Xia, Q., Liu, M., Zhang, X., Jin, L., & Zhang, C. (2025). Machine learning-guided optimization of high-performance porous composite membranes for alkaline water electrolysis. Energy and AI, 22, Article 100657. https://doi.org/10.1016/j.egyai.2025.100657